Cyclic Behavior and Seismic Design of Bolted Flange Plate Steel Moment Connections

ATSUSHI SATO, JAMES D. NEWELL and CHIA-MING UANG

Steel moment connections in high seismic regions typically use welded beam flange-to-column flange joints. Field welding of these connections has significant economic impact on the overall cost of the building. A moment connection that could eliminate field welding in favor of field bolting and shop welding could result in a more economical seismic moment frame connection.

One type of bolted moment frame connection consists of plates that are shop welded to the column flange and field bolted to the beam flange and is known as the bolted flange plate (BFP) moment connection. As a part of the SAC Joint Venture Phase II Connection Performance Program, eight full-scale BFP moment connection specimens were tested (Schneider and Teeraparbwong, 2000). Tested connections exhibited predictable, ductile behavior and met established acceptance criteria. However, beam sizes were limited to W24×68 and W30×99.

The AISC Connection Prequalification Review Panel (CPRP) is currently reviewing the bolted flange plate moment connection for inclusion in the next edition of the AISC *Prequalified Connections for Special and Intermediate Steel Moment Frames for Seismic Applications* (AISC 2005a). To expand the experimental database for prequalifying the BFP moment connection for special moment frames, cyclic testing of three full-scale BFP steel moment connection specimens has been conducted. Beam sizes for these specimens (W30×108, W30×148, and W36×50) were larger than previously tested to extend the range of available experimental results.

Atsushi Sato is assistant professor, department of architecture and architectural engineering, Kyoto University, Kyoto, Japan, and formerly visiting scholar, department of structural engineering, University of California, San Diego, La Jolla, CA.

James D. Newell is graduate student researcher, department of structural engineering, University of California, San Diego, La Jolla, CA.

Chia-Ming Uang is professor, department of structural engineering, University of California, San Diego, La Jolla, CA.

EXPERIMENTAL PROGRAM

Connection Details and Test Setup

Three full-scale, one-sided moment connection specimens, without a concrete slab were fabricated and tested in accordance with Appendix S of the AISC *Seismic Provisions for Structural Steel Buildings*, hereafter referred to as the AISC *Seismic Provisions* (AISC, 2005b). Specimens were designed in accordance with the design procedure developed by the BFP Committee of AISC's CPRP. The design procedure (see Appendix I) assumes the beam plastic hinge is located at the center of the outermost (farthest from the column face) row of bolts. Tables 1a and 1b list the member sizes and connection details for the specimens. Beam-to-column connection details are shown in Figure 1. As indicated in Table 1, Specimens BFP-1 and BFP-2 had 1 in. continuity plates and Specimen BFP-3 did not have continuity plates. Specimen BFP-1 did not have a panel zone doubler plate while Specimens BFP-2 and BFP-3 included a ¾-in. doubler plate.

Bolt holes in the beam shear tab were short-slotted with the slot length oriented parallel to the beam span and bolt holes in the beam web were standard holes. Bolt holes in the flange plate were oversized holes (1¼-in. diameter for 1-in. diameter bolts) and bolt holes in the beam flange were standard holes (1¹⁄₁₆-in. diameter for 1-in. diameter bolts). The short-slotted holes in the shear tab and oversized holes in the flange plate were provided to accommodate erection tolerances.

The distance between the two bolted flange plates was detailed to be ⅜ in. larger than the nominal beam depth. This tolerance accommodates typical variations in actual beam depth and any gaps between the beam flange and flange plate larger than ⅛ in. are filled with finger shims. For all specimens, two ⅛-in. finger shim plates (total ¼ in.) were installed between the top flange plate and beam top flange. No shims were used between the bottom flange plate and beam bottom flange.

The clear-bay-width to beam-depth ratio of previously tested BFP moment connection specimens varied from approximately 9 to 12 (Schneider and Teeraparbwong, 2000). For Specimens BFP-1, BFP-2 and BFP-3 the beam length varied in order to maintain a target clear-bay-width to beam-depth ratio of 12. The overall specimen geometry and test setup is shown in Figure 2. Simulated pins were provided at the ends of the column, and actuator attachment point at the

Table 1a. Member Sizes				
Specimen Designation	Column	Beam	L_c (in.)	L_c/d_b[a]
BFP-1	W14×233	W30×108	355¾	11.94
BFP-2	W14×233	W30×148	367½	11.97
BFP-3	W14×311	W36×150	426⅞	11.89

[a] Clear bay width-to-beam depth ratio, L_c/d_b (target ratio = 12)

Table1b. Connection Details					
Specimen Designation	Flange Plates (in.)	Flange Plate Welding	Row of Bolts	Panel Zone Doubler Plate (in.)	Continuity Plates (in.)
BFP-1	1½	ESW	7	NA	1
BFP-2	1¾	ESW	11	¾	1
BFP-3	1¾	FCAW	10	¾	NA

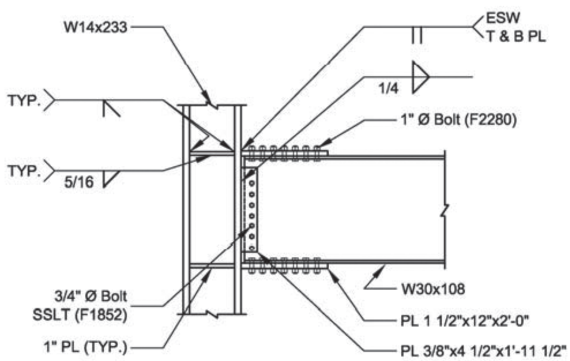

(a) Specimen BFP-1

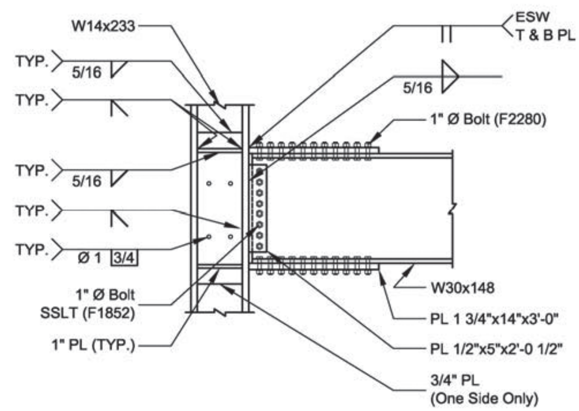

(b) Specimen BFP-2

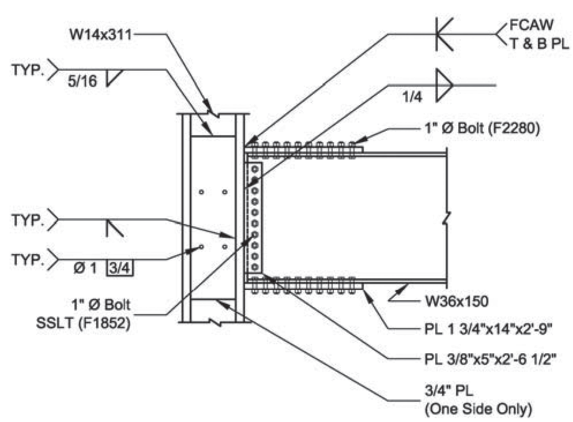

(c) Specimen BFP-3

Fig. 1. Moment connection details.

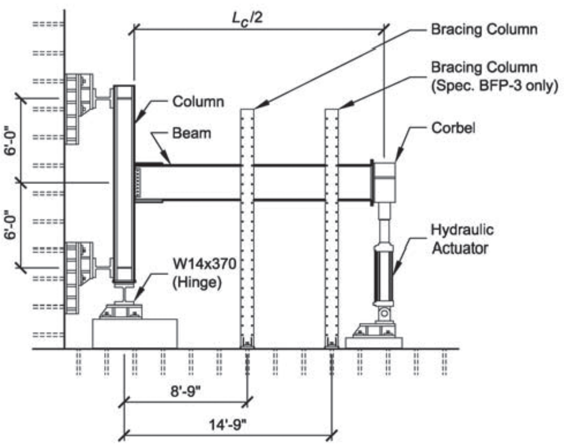

(a) Schematic

(b) Specimens BFP-1 and BFP-2

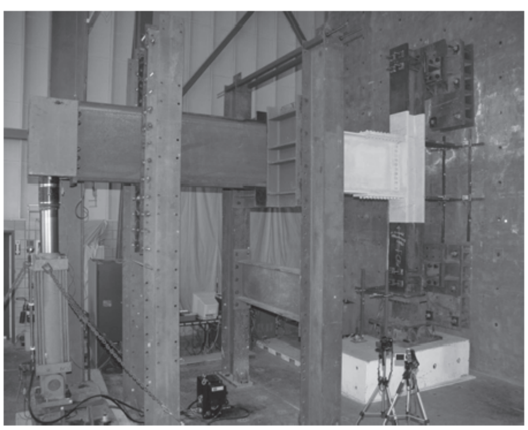

(c) Specimen BFP-3

Fig. 2. Test setup.

end of the beam to simulate inflection points in the actual building. A load transfer corbel was bolted to the end of the beam and attached to a servo-controlled hydraulic actuator.

The maximum lateral bracing spacing permitted by the AISC *Seismic Provisions* for Specimens BFP-1, BFP-2 and BFP-3 was 107, 113 and 123 in., respectively. For Specimens BFP-1 and BFP-2 lateral bracing of the beam was provided approximately 105 in. from the centerline of the column. The same lateral bracing at a distance of 105 in. from the column was also used for Specimen BFP-3. But since testing of both Specimens BFP-1 and BFP-2 showed significant beam lateral-torsional buckling and column twisting, it was decided to add additional lateral bracing at 177 in. from the column centerline (see Figure 2).

Fabrication and Erection

Two different welding processes were used for the flange-plate to column-flange complete joint penetration groove welds. Flange plates were welded to the column using the electroslag welding (ESW) process for Specimens BFP-1 and BFP-2 and using the flux-cored arc welding (FCAW) process for Specimen BFP-3.

For the ESW flange-plate to column-flange welds the sides of the weld were formed by water-cooled copper shoes. Two Arcmatic 105-VMC 3/32 in. diameter electrodes were placed inside a consumable guide tube. Flux (FES72) was added by hand per the fabricator's standard procedure. It took approximately 15 minutes to completely weld each flange plate. The electrode used has a specified minimum Charpy-V notch (CVN) toughness of 15 ft-lb at −20 °F. [AISC *Seismic Provisions* specifies a minimum CVN toughness of 20 ft-lb at −20 °F and 40 ft-lb at 70 °F for demand critical welds. On the other hand, American Welding Society (AWS) *Structural Welding Code–Seismic Supplement*, AWS D1.8 (AWS, 2005) specifies a minimum CVN toughness of 20 ft-lb at 0 °F and 40 ft-lb at 70 °F for demand critical welds.]

FCAW of the flange plates to the column flange was done with an E70T-1 gas-shielded flux-cored electrode (Hobart Brothers TM-11, 3⁄32-in. diameter) and 100% CO_2 shielding gas. This electrode has a specified minimum CVN toughness of 20 ft-lb at 0 °F.

Welding of continuity plates and panel zone doubler plates for all specimens used the FCAW process. Welding was done with an E70T-1/E70T-9 gas-shielded flux-cored electrode (Lincoln Outershield 70, 3⁄32-in. diameter) and 100% CO_2 shielding gas. This electrode has a specified minimum CVN Toughness of 20 ft-lb at −20 °F.

Specimens were erected at University of California, San Diego, by laboratory staff. The column was first placed in position in the test setup, followed by installation of the beam to simulate the field erection process. Beam web to shear tab bolts were ASTM F1852 (A325TC) tension control bolts. Flange plate to beam flange bolts were

Table 2. Steel Mechanical Properties

Member	Size	Steel Grade	Yield Strength[a] (ksi)	Tensile Strength[a] (ksi)	Elongation[a,b] (%)
Column	W14×233	A992	51.5	76.5	28
	W14×311		55.0	78.0	27
Beam	W30×108		52.0	77.5	30
	W30×148		58.5	80.0	27
	W36×150		63.5	81.0	31
Bolted Flange Plate	1½-in. PL	A572 Gr. 50	60.5	87.5	25
	1¾-in. PL		54.5	81.5	27
Doubler Plate	¾ in. PL		(57.0)	(78.0)	(20)
Continuity Plate	1 in. PL		(56.7)	(80.3)	(20)

[a] Values in parentheses are based on Certified Mill Test Reports.
[b] Certified Mill Test Report elongation in parentheses based on 8-in. gage length, others based on 2-in. gage length.

ASTM F2280 (A490TC) tension control bolts. Bolts were initially brought to the snug-tight condition with connected plies in firm contact followed by systematic tensioning of the bolts. For the beam web to shear tab connection the middle bolt was tensioned first and then bolts were tensioned outward from the middle progressing in an alternating up and down pattern. Flange plate to beam flange bolts were tensioned, starting with the most rigid portion of the connection near the face of the column and then working progressively outward.

Material Properties

ASTM A992 steel was specified for all beam and column members. ASTM A572 Gr. 50 steel was specified for all plate material. Material properties determined from tension coupon testing are shown in Table 2 and additional information may be found in Sato, Newell and Wang (2008).

Loading Protocol and Instrumentation

The loading sequence for beam-to-column moment connections as defined in the 2005 AISC *Seismic Provisions* was used for testing (see Figure 3). Displacement was applied at the beam tip and was controlled by the interstory drift angle. Specimens were instrumented with a combination of displacement transducers, strain gage rosettes, and uniaxial strain gages to measure global and local responses. Figure 4 shows the location of displacement transducers. Displacement transducer δ_{total} measured the overall vertical displacement of the beam tip. δ_1 and δ_2 measured column movement. δ_3 and δ_4 measured the average shear deformation of the column panel zone. δ_5 and δ_6 measured the slippage between flange plates and beam flanges. For additional instrumentation information see Sato et al. (2008). The data reduction procedure was a modified version of one formulated by Uang and Bondad (1996). The procedure (see Appendix II) was used to compute the components of beam tip displacement, δ_{total}, that are contributed by deformation of the beam, column, panel zone and slip-bearing between the flange plates and beam flanges.

EXPERIMENTAL RESULTS

Several observations were made during testing that were similar for all three specimens. Bolt slip, which produced very loud noises, occurred during early cycles (at 0.375% or 0.5% drift) and on all subsequent cycles. Yielding in the connection region, as evidenced by flaking of the whitewash, was observed to initiate at 2% drift. Beam flange and web local buckling initiated at 4% drift, and lateral-torsional buckling (LTB) of the beam together with twisting of the column was observed at 5% drift.

Testing of Specimen BFP-2 was stopped after one complete cycle at 6% drift due to safety concerns resulting from the observed column twisting [see Figure 5(a)]. For Specimen BFP-3 significant beam LTB and column twisting, as shown in Figure 5(b), were observed at 6% drift. For this specimen, which did not require continuity plates, the unusual yielding pattern of the column, shown in Figure 6, might have been caused by column flange local bending, web local yielding, and column twisting (i.e., warping stress).

Specimen BFP-1 experienced net section fracture of the beam bottom flange at the outermost bolt row on the second excursion to 6% drift. Specimen BFP-3 failed in the same

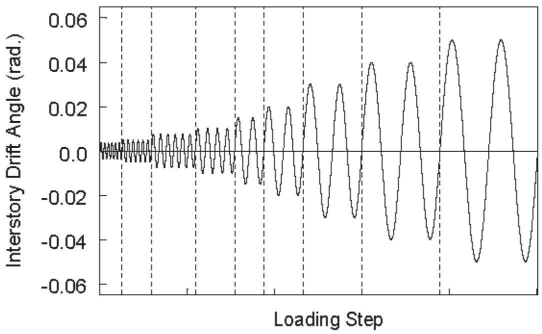

Fig. 3. AISC loading sequence.

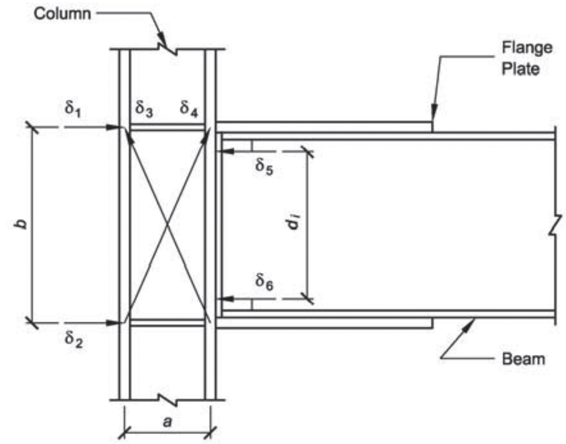

Fig. 4. Instrumentation plan.

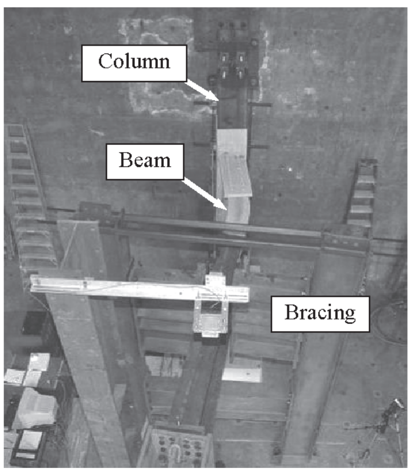

(a) Specimen BFP-2

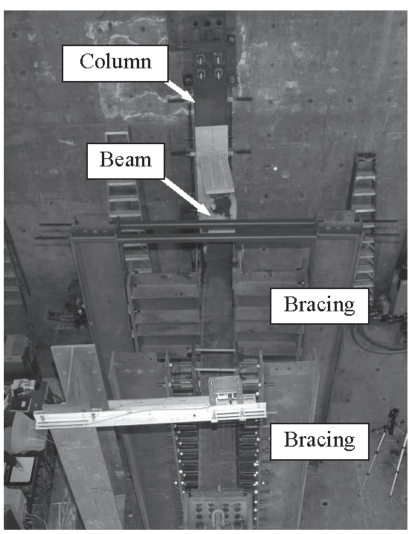

(b) Specimen BFP-3

Fig. 5. Beam lateral-torsional buckling and column twisting at 6% drift.

(a) Overall (west side)

(b) West side detail

(c) East side detail

Fig. 6. Specimen BFP-3: yielding in column.

manner on the first excursion to 7% drift. Figure 7 shows the location and a close-up view of the fracture. For both specimens LTB of the beam increased the tensile strain demand on the edge of the flange net section (i.e., between the flange edge and bolt hole) where failure was observed. Maintaining an adequate edge distance is, therefore, important for the design of BFP connections. Fracture was preceded by the occurrence of necking at the net section. It is likely that Specimen BFP-2 would have experienced net section fracture had testing not been stopped due to safety concerns.

A plot of the moment (at column face) versus beam tip displacement relationship is shown in Figure 8 for the three specimens. To meet the acceptance criteria of the AISC *Seismic Provisions*, specimens shall satisfy the following requirements: (1) the connection must be capable of sustaining an interstory drift angle of at least 0.04 rad, and (2) the required flexural strength of the connections, determined at the column face, must equal at least 80% of the nominal plastic moment (M_{pn}) of the connected beam at an interstory drift angle of 0.04 rad. The vertical dashed lines shown in Figure 8 are at 4% drift and the horizontal dashed lines are at 80% of the nominal plastic moment. Specimens exceeded the requirements of the AISC acceptance criteria and achieved an interstory drift angle of at least 0.06 rad. The pinching observed in the hysteresis loops is mainly attributed to the slip-bearing behavior of the bolted connection. After some amount of initial slippage, hardening behavior can be observed due to bearing between the bolt, flange plate and beam flange.

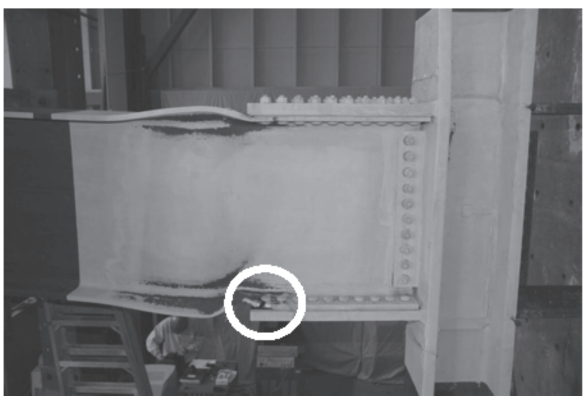

(a) Fracture Location

(b) Close-up

Fig. 7. Specimen BFP-3: beam flange net section fracture.

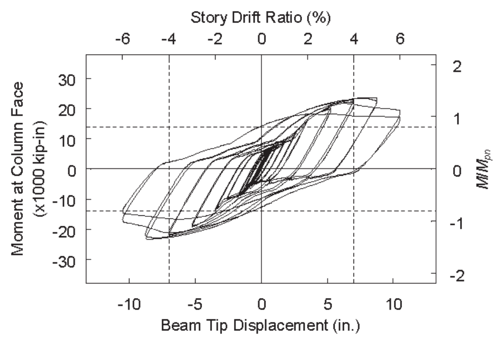

(a) Specimen BFP-1

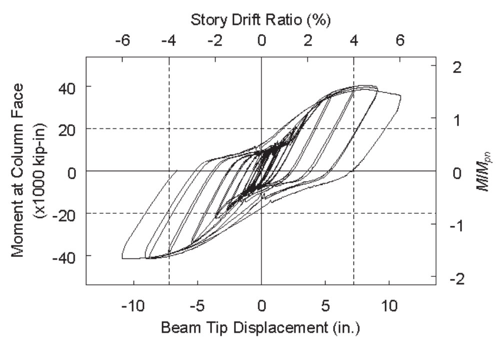

(b) Specimen BFP-2

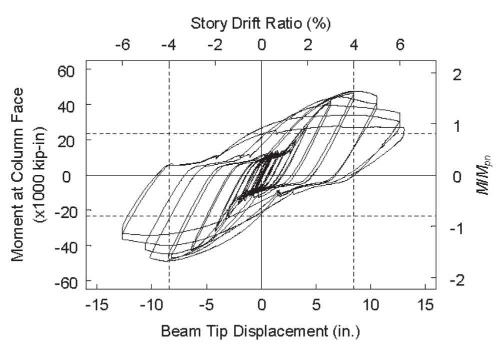

(c) Specimen BFP-3

Fig. 8. Moment versus beam tip displacement relationships.

Figure 9 shows the relative contribution of the column, beam, panel zone, and slip-bearing deformation to the overall beam tip displacement at different drift levels. [For Specimen BFP-2, components at 5% and 6% drift are not shown in Figure 9(b) because column twisting affected the measurements.] Shear deformation in the panel zone and slippage between the flange plate and beam flange made significant contributions to the total beam tip displacement of Specimens BFP-1 and BFP-2. Deformation in the panel zone of Specimen BFP-3 was limited because of the strong panel zone (demand-capacity ratio of 0.73). But slippage and bearing between the flange plate and beam flange made a significant contribution to the total beam tip displacement.

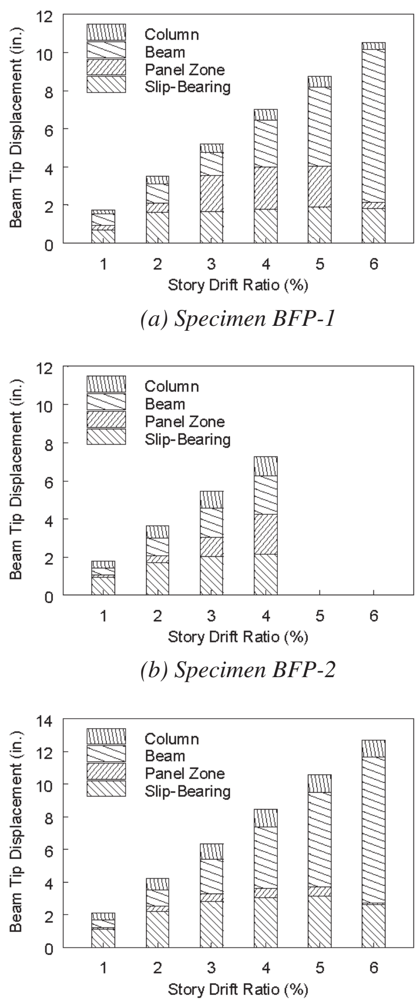

(a) Specimen BFP-1

(b) Specimen BFP-2

(c) Specimen BFP-3

Fig. 9. Components of beam tip displacement.

COMPARISON OF RESULTS

The overstrength factor, α, resulting from cyclic strain hardening, for each specimen as computed from Equation 1 is shown in Figure 10.

$$\alpha = \frac{M_u}{M_{pa}} \tag{1}$$

Ultimate moment, M_u, was calculated from test data at the assumed plastic hinge location and M_{pa} was the plastic moment of the beam based on measured flange yield strength. Specimen overstrength values were similar to the value of 1.15 [= $(F_y + F_u)/2F_y$] given by AISC *Prequalified Connections for Special and Intermediate Steel Moment Frames for Seismic Applications* (AISC, 2005a).

Significant LTB of the beam and twisting of the column were observed in all specimens. Figure 11(b) shows one column flange strain gauge, near the flange tip, plotted versus the gauge near the opposite flange tip [see Figure 11(a)] for Specimen BFP-2. Deviation from the one-to-one (dashed) line provides an indication of column twisting (i.e., warping stress). Similar evidence of column twisting was observed for the other specimens. The specimens did not include a concrete structural slab, which would have provided lateral bracing to the beam top flange and torsional restraint to the column. Column twisting has been observed in testing of RBS moment connection specimens with deep columns and without a concrete structural slab (Chi and Uang, 2002), but not in testing with W14 columns. Additional deep column moment connection testing has indicated that the presence of a concrete structural slab mitigates column twisting issues associated with deep columns (Zhang and Ricles, 2006). However, the column twisting observed in this testing is a phenomenon that has not been previously observed in testing of moment connections with W14 columns with or without a concrete structural slab.

Potential contributing factors to the observed column twisting include (1) the geometry of the flange plate connection, which pushes the plastic hinge location further away from the column face, and (2) the oversized holes in

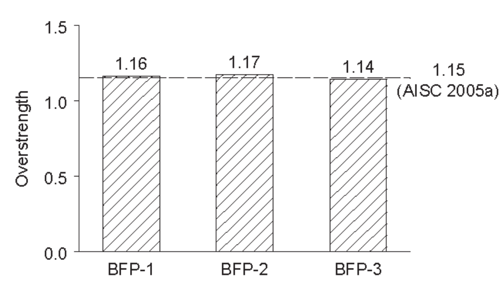

Fig. 10. Beam cyclic overstrength ratio.

the flange plates allowing transverse movement of the beam. The gap between oversized bolt holes and the bolt shank allows for transverse movement of the beam; the second-order effect resulting from such eccentricity in the beam compression flange, although small initially, promotes LTB of the beam. With the plastic hinge located farther away from the column face than for typical (e.g., reduced beam sections) welded moment connections, the effect of out-of-plane forces is magnified (Chi and Uang, 2002).

It is expected based on the design of the bolted connection that slip will occur. However, slip occurred at approximately one-half the expected slip capacity considering the total resistance of all bolts in the connection. As shown in Figure 9, deformation from slip-bearing made a significant contribution to the total deformation. For all specimens at 4% drift slip-bearing deformation contributed approximately 30% of the total deformation. The level of slip-bearing deformation was observed to be consistent for different loading amplitudes (i.e., 2, 3, 4%, drift).

The contribution of slip-bearing deformation to the total deformation is dependent on the oversize of the bolt holes in the flange plate and beam flange. During testing, bolt slip was observed to occur on early cycles and significantly contributed to the overall beam tip displacement on these cycles. As a result, beam flange yielding for the BFP specimens was not observed to occur until 2% drift, whereas for a typical welded moment connection, flange yielding would be expected at about 1% drift. Also, the observed level of beam flange and web local buckling was less severe than observed in previous testing of welded moment connections (Uang, Yu, Noel and Gross, 2000). Bolt slippage and bearing deformation in the BFP connection accommodated deformation that would have induced both local and lateral-torsional buckling in a welded connection.

Specimens BFP-1 and BFP-3 eventually failed by net section fracture of the beam flange at the outermost row of bolts. Testing of Specimen BFP-2 was stopped before fracture, but necking at the outermost row of bolts was observed and it is likely that fracture on the net section would have occurred if testing was continued. Demand on the net section was exacerbated by LTB of the beam. Figure 12 shows strain profiles across the Specimen BFP-3 beam bottom flange for different drift levels. The skew of the strain profiles at higher drift levels resulted from beam LTB.

SUMMARY AND CONCLUSIONS

Three full-scale, one-sided, bolted flange plate steel moment-frame connection specimens consisting of W14 columns and W30 to W36 beams were subjected to increasing amplitude cyclic testing to support prequalification of the bolted flange plate connection for special moment resisting frames. All three specimens performed well and met the acceptance criteria of the AISC *Seismic Provisions*.

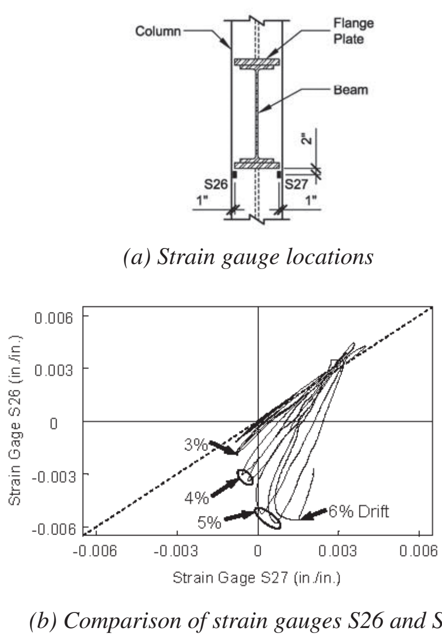

(b) Comparison of strain gauges S26 and S27

Fig. 11. Specimen BFP-2: column flange strains.

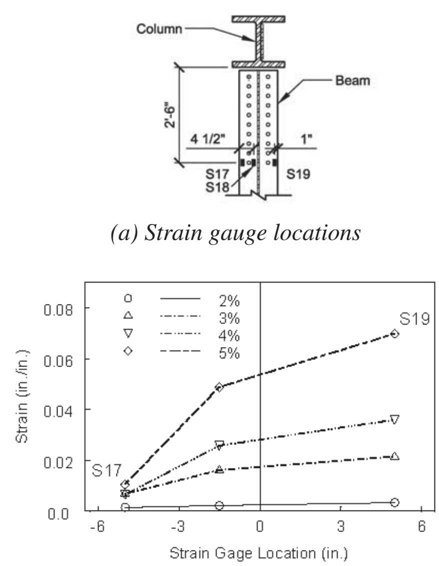

(a) Strain profile (S17, S18, S19)

Fig. 12. Specimen BFP-3: strain profiles across beam bottom flange.

Specimens achieved an interstory drift angle of 0.06 rad before failure. Specimens BFP-1 and BFP-3 failed by beam flange net section fracture and for Specimen BFP-2 necking at the outermost row of bolts was observed. The tensile demand on the net section where fracture occurred was further increased by LTB of the beam.

On large drift cycles (5% and 6%) column twisting was observed in addition to beam LTB. The specimens did not include a concrete structural slab, which would limit LTB and column twisting. However, column twisting has not previously been observed in testing of moment connection specimens with W14 columns without a concrete structural slab.

Bolt-slip occurred early during testing of all three specimens. The BFP connection differs from welded moment connections in that the additional component of bolt slip-bearing contributes to overall inelastic deformation of the connection. Slip-bearing deformation contributed a significant amount to the total deformation (approximately 30% of the total deformation at 4% drift).

ACKNOWLEDGMENTS

Funding for this project was provided by the American Institute of Steel Construction; Mr. Tom Schlafly was the project manager. Design of the test specimens was provided by Professor Linda Hanagan of Pennsylvania State University. Materials and fabrication were donated by Schuff Steel Company and Nucor Fastener.

APPENDIX I: DESIGN PROCEDURE

The draft design procedure outlined below has been developed by AISC's CPRP BFP Committee for inclusion in Supplement Number 1 to *Prequalified Connections for Special and Intermediate Steel Moment Frames for Seismic Applications,* hereafter referred to as AISC *Prequalified Connections* (ANSI/AISC 358-05). The design procedure assumes the beam plastic hinge is located at the center of the outermost (furthest from the column face) row of bolts. The required number of bolts is determined from the force in the flange plates due to the expected moment demand at the face of the column. Controlling shear strength per bolt is determined considering the limit states of bolt shear strength and bearing strength on the beam flange and flange plate. Tensile rupture of the flange plate and block shear of the beam flange are checked. Continuity plate and column panel zone requirements are similar to typical special moment frame requirements.

1. Compute the probable maximum moment at the beam hinge using the requirements of AISC *Prequalified Connections* Section 2.4.3.

$$M_{pr} = C_{pr} R_y F_y Z_x \tag{A-1}$$

2. Compute the maximum bolt diameter preventing beam flange tensile rupture. For standard holes with two bolts per row:

$$d_b \le \frac{b_f}{2}\left(1 - \frac{R_y F_y}{R_t F_u}\right) - \frac{1}{8}\text{ in.} \tag{A-2}$$

3. Considering bolt shear and bolt bearing, determine the controlling nominal shear strength per bolt.

$$r_n = \min\begin{Bmatrix} 1.1 A_b F_{nv} \\ 2.4 d_b t_f F_{ub} \\ 2.4 d_b t_p F_{up} \end{Bmatrix} \tag{A-3}$$

4. Select a trial number of bolts. The following equation may be a useful way of estimating the trial number of bolts.

$$n \ge \frac{1.25 M_{pr}}{\phi_n r_n (d + t_p)} \tag{A-4}$$

5. Determine the beam plastic hinge location, as dimensioned from the face of the column.

$$S_h = S_1 + s\left(\frac{n}{2} - 1\right) \tag{A-5}$$

The bolt spacing between rows, s, and the edge distance shall be large enough to ensure that L_c, as defined in AISC *Specification* (AISC, 2005c) Section J3.10, is greater than or equal to $2d_b$.

6. Compute the shear force at the beam plastic hinge location at each end of the beam. The shear force at the hinge location, V_h, shall be determined by a free body diagram of the portion of the beam between the hinge locations. This calculation shall assume the moment at the hinge location is M_{pr} and shall include gravity loads acting on the beam based on the load combination, $1.2D + f_1 L + 0.2S$.

7. Calculate the moment expected at the face of the column flange.

$$M_f = M_{pr} + V_h S_h \tag{A-6}$$

8. Compute the force in the flange plate due to M_f.

$$F_{pr} = \frac{M_f}{\left(d + t_p\right)} \tag{A-7}$$

9. Confirm that the number of bolts selected in Step 4 is adequate.

$$n \geq \frac{F_{pr}}{\phi_n r_n} \tag{A-8}$$

10. Determine the required thickness of the flange plate.

$$t_p \geq \frac{F_{pr}}{\phi_d F_y b_{fp}} \tag{A-9}$$

11. Check the flange plate for tensile rupture.

$$F_{pr} \leq \phi_n R_n \tag{A-10}$$

where R_n is defined in AISC *Specification* Section J4.1.

12. Check the beam flange for block shear.

$$F_{pr} \leq \phi_n R_n \tag{A-11}$$

where R_n is defined in AISC *Specification* Section J4.3.

13. Check the flange plate for compression buckling.

$$F_{pr} \leq \phi_n R_n \tag{A-12}$$

where R_n is defined in AISC *Specification* Section J4.4. When checking compression buckling of the flange plate, the effective length, KL, may be taken as $0.65S_1$.

14. Determine the required shear strength, V_u, of beam and beam web-to-column connection from:

$$V_u = \frac{2M_{pr}}{L'} + V_{gravity} \tag{A-13}$$

Check design shear strength of beam according to Chapter G of the AISC *Specification*.

15. Design a single plate shear connection for the required strength, V_u, calculated in Step 14 and located at the face of the column, meeting the limit state requirements of the AISC *Specification*.

16. Check the continuity plate requirements according to Chapter 2 of AISC *Prequalified Connections*.

17. Check the column panel zone according to Section 9.3 or 10.3 of the AISC *Seismic Provisions*, as appropriate. The required shear strength of the panel zone shall be determined from the summation of the moments at the column faces as determined by projecting moments equal to $R_y F_y Z_x$ at the plastic hinge points to the column faces. Add twice the thickness of the flange plate to the beam depth for determining the value of d.

18. Check the column-beam moment ratio according to Section 9.6 or 10.6 of the AISC *Seismic Provisions*, as appropriate.

APPENDIX II: DATA REDUCTION PROCEDURE

1. Panel Zone Component: Use Equation A-14 to compute the average panel zone shear strain, $\bar{\gamma}$, and Equation A-15 to compute the panel zone deformation contribution, δ_{pz}, to total beam tip displacement, δ_{total}.

$$\bar{\gamma} = \frac{\sqrt{a^2 + b^2}}{2ab}\left(\delta_3 - \delta_4\right) \tag{A-14}$$

$$\delta_{pz} = \bar{\gamma} L_b \tag{A-15}$$

2. Column Component: The column rotation, θ_c, can be computed from Equation A-16 and the column deformation contribution, δ_c to δ_{total}, from Equation A-17.

$$\theta_c = \frac{\left(\delta_2 - \delta_1\right)_{total}}{d_b} - \bar{\gamma}\left(1 - \frac{d_b}{H}\right) \tag{A-16}$$

$$\delta_c = \theta_c \left(L_b + \frac{d_c}{2}\right) \tag{A-17}$$

3. Slip-Bearing Component: The slip-bearing rotation, θ_{SB}, and slip-bearing beam tip displacement component, δ_{SB}, can be computed from Equations A-18 and A-19, respectively.

$$\theta_{SB} = \frac{\left(\delta_5 - \delta_6\right)}{d_i} \tag{A-18}$$

$$\delta_{SB} = \theta_{SB} L \tag{A-19}$$

4. Beam Component: The beam component, δ_b of δ_{total}, can be computed from Equation A-20.

$$\delta_b = \delta_{total} - \delta_{pz} + \frac{\bar{\gamma} d_b}{H}\left(L_b + \frac{d_c}{2}\right) - \delta_c - \delta_{SB} \tag{A-20}$$

NOTATION

A_b Nominal unthreaded body area of bolt

C_{pr} Factor to account for peak connection strength, including strain hardening, local restraint, additional reinforcement, and other connection conditions

D Nominal dead load

F_{nv} Nominal shear stress from AISC *Specification* Table J3.2

F_{pr} Probable maximum flange plate force

F_u Specified minimum tensile strength

F_y Specified minimum yield stress

F_{ub} Specified minimum tensile strength of beam material

F_{up} Specified minimum tensile strength of plate material

H Column height

L Nominal live load

L' Distance between hinge locations

L_b Beam clear length

L_c Clear bay width

L_c Clear distance, in the direction of the force, between the edge of the hole and the edge of the adjacent hole or edge of the material

M_f Expected moment at the face of the column flange

M_{pa} Actual plastic moment of the beam

M_{pn} Nominal plastic moment of the beam

M_{pr} Probable maximum moment at plastic hinge

M_u Ultimate moment of the beam achieved at assumed plastic hinge location (outermost row of bolts)

R_n Nominal strength

R_t Ratio of the expected tensile strength to the specified minimum tensile strength F_u

R_y Ratio of the expected yield stress to the specified minimum yield stress F_y

S Snow load

S_1 Distance from face of column to the first row of bolts

S_h Distance from face of column to the plastic hinge location

$V_{gravity}$ Beam shear force resulting from $1.2D + f_1L + 0.2S$

V_h Larger of the two values of shear force at the beam hinge location at each end of the beam

V_u Required shear strength of beam and beam web to column connection

Z_x Plastic section modulus of a member

a Panel zone width

b Panel zone depth

b_f Width of beam flange

b_{fp} Width of flange plate

d Beam depth

d_b Beam depth

d_b Nominal bolt diameter

d_c Column depth

d_i Distance between displacement transducers δ_5 and δ_6

f_1 Load factor determined by the applicable building code for live loads, but not less than 0.5

n Number of bolts

r_n Nominal strength

s Bolt spacing between rows

t_f Beam flange thickness

t_p Flange plate thickness

α Overstrength factor accounting for cyclic strain hardening

δ_1, δ_2 Column displacement transducer (see Figure 4)

δ_3, δ_4 Panel zone displacement transducer (see Figure 4)

δ_5, δ_6 Slip-bearing displacement transducer (see Figure 4)

δ_b Beam component of δ_{total}

δ_c Column component of δ_{total}

δ_{pz} Panel zone component of δ_{total}

δ_{SB} Slip-bearing component of δ_{total}

δ_{total} Total beam tip displacement

θ_c Column rotation

θ_{SB} Slip-bearing rotation

ϕ_d Resistance factor for ductile limit states

ϕ_n Resistance factor for non-ductile limit states

$\bar{\gamma}$ Average panel zone shear strain

REFERENCES

AISC (2005a), ANSI/AISC 358-05, *Prequalified Connections for Special and Intermediate Steel Moment Frames for Seismic Applications*, American Institute of Steel Construction, Chicago, IL.

AISC (2005b), ANSI/AISC 341-05, *Seismic Provisions for Structural Steel Buildings,* American Institute of Steel Construction, Chicago, IL.

AISC (2005c), ANSI/AISC 360-05, *Specification for Structural Steel Buildings,* American Institute of Steel Construction, Chicago, IL.

AWS (2005), *Structural Welding Code—Seismic Supplement*, AWS D1.8, American Welding Society, Miami, FL.

Chi, B. and Uang, C.M. (2002), "Cyclic Response and Design Recommendations of Reduced Beam Section Moment Connections with Deep Columns," *Journal of Structural Engineering*, ASCE, Vol. 128, Issue 4, pp. 464–473.

Schneider, S. and Teeraparbwong, I. (2000), *Bolted Flange Plate Connections*, *Report No. SAC/BD-00/05*, SAC Joint Venture, Sacramento, CA.

Sato, A., Newell, J. and Uang, C.M. (2008), *Cyclic Testing of Bolted Flange Plate Steel Moment Connections for Special Moment Frames, Report No. SSRP-07/10*, Department of Structural Engineering, University of California, San Diego, La Jolla, CA.

Uang, C.M. and Bondad, D. (1996), *Static Cyclic Testing of Pre-Northridge and Haunch Repaired Steel Moment Connections, Report No. SSRP-96/02*, Division of Structural Engineering, University of California, San Diego, La Jolla, CA.

Uang, C.M., Yu, Q.S., Noel, S. and Gross, J. (2000), "Cyclic Testing of Steel Moment Connection Rehabilitated with RBS or Welded Haunch," *Journal of Structural Engineering*, ASCE, Vol. 126, Issue 1, pp. 57–68.

Zhang, X. and Ricles, J. (2006), "Experimental Evaluation of Reduced Beam Section Connections to Deep Columns," *Journal of Structural Engineering*, ASCE, Vol. 132, Issue 3, pp. 346–357.